*Journal of Applied Fluid Mechanics*, Vol. 9, No. 6, pp. 2855-2864, 2016.
Available online at www.jafmonline.net, ISSN 1735-3572, EISSN 1735-3645.
DOI: 10.29252/jafm.09.06.26060

# Effect of Radial Magnetic Field on Free Convective Flow over Ramped Velocity Moving Vertical Cylinder with Ramped Type Temperature and Concentration

V. Vanita and A. Kumar†

*Department of Mathemmatics, Central University of Rajasthan, Ajmer, India*

†*Corresponding Author Email: aanandbhu@gmail.com*

(Received December 30, 2015; accepted April 15, 2016)

## ABSTRACT

A numerical study has been performed to analyze the effect of radial magnetic field on free convective flow of an electrically conducting and viscous incompressible fluid over the ramped moving vertical cylinder with ramped type temperature and concentration considered at the surface of vertical cylinder. The governing partial differential equations which describe the flow formation have been solved numerically by using implicit finite difference method of Crank-Nicolson type. The simulation results of the considered model have been shown graphically. One of the interesting result of our analysis is that the local as well as average skin-friction, Nusselt number and Sherwood number have increasing tendency in time interval (0,1), thereafter these quantities decrease. We have also compared the case of ramped type boundary conditions with that of constant boundary conditions with help of table. The advantage of taking ramped type boundary conditions is that initial heat transfer rate and mass transfer rate are minimum in this case.

**Keywords:** Ramped velocity; Ramped temperature; Ramped concentration; Radial magnetic field; Magnetic parameter; Vertical cylinder.

## NOMENCLATURE

| | |
|---|---|
| $B_0$ | radial magnetic field |
| $C'$ | species concentration |
| $C$ | dimensionless species concentration |
| $D$ | mass diffusion coefficient |
| $g$ | acceleration due to gravity |
| $Gr$ | Thermal Grashof number |
| $Gc$ | Mass Grashof number |
| $M$ | Magnetic parameter |
| $Nu$ | Local Nusselt number |
| $Nu_{av}$ | Average Nusselt number |
| Pr | Prandtl number |
| $r_0$ | characteristic radius |
| $r$ | radial coordinate |
| $R$ | dimensionless radial coordinate |
| $Sc$ | Schmidt number |
| $Sh$ | Sherwood number |
| $Sh_{av}$ | average Sherwood number |
| $T'$ | temperature |
| $T$ | dimensionless temperature |
| $t'$ | time |
| $t$ | dimensionless time |
| $t_0$ | characteristic time |
| $u$ | velocity component in x-direction |
| $u_0$ | characteristic velocity |
| $v$ | velocity component in r-direction |
| $U$ | dimensionless velocity component in x-direction |
| $V$ | dimensionless velocity component in r-direction |
| $x$ | axial coordinate |
| $X$ | dimensionless axial coordinate |
| $\alpha$ | thermal diffusivity |
| $\beta_T$ | volumetric coefficient of thermal expansion |
| $\beta_C$ | volumetric coefficient of solutal expansion |
| $\sigma$ | conductivity |
| $\nu$ | kinematic viscosity |
| $\rho$ | density |
| $\tau$ | local skin-friction |
| $\tau_{av}$ | average skin-friction |

**subscripts**

| | |
|---|---|
| $w$ | at the wall |
| $\infty$ | at free stream |

## 1. INTRODUCTION

Free convection flow involving heat and mass transfer simultaneously, have shown wide appearance in practical as well as in industrial situations like evaporation, condensation, formation and dispersion of fog, ocean circulations, thermal insulation, enhanced oil recovery etc. In industries, many transport processes are observed in which simultaneous heat and mass transfer occurs as a result of combined buoyancy effects of temperature difference and concentration difference. Since, cylinders have been used in nuclear waste disposal, underground energy extortion, cooling of nuclear reactors and catalytic bed reactors, therefore the convective heat and mass transfer about cylindrical bodies has gained the attention of many researchers. Sparrow and Gregg (1956) were the first, who studied the heat transfer from vertical cylinders. Yang (1960) performed an analysis of the unsteady laminar boundary-layer equations for free convection on vertical plates and cylinders and he derived necessary conditions for feasibility of similarity solutions. The combined heat and mass transfer in natural convection along vertical cylinder for both conditions of uniform wall temperature or concentration and uniform heat or mass flux was investigated by Chen and Yuh (1980). Lien *et al*. (1985) have contemplated the isothermal and constant heat flux cases for the free convective flow past an impulsively moving infinite vertical circular cylinder.

Gorla (1989) presented a numerical solution of combined forced and free convection in the boundary layer flow of a micropolar fluid on a continuous moving vertical cylinder. He noticed that the wall shear stress and surface heat transfer rate increase with increasing buoyancy force and increasing transverse curvature of the surface. Velusamy and Grag (1992) gave a numerical solution for the transient natural convection over a heat generating vertical cylinder. Ganesan and Rani (1998) considered the transient natural convection along vertical cylinder with heat and mass transfer and they concluded that with increase in Schmidt number steady state reaches later while buoyancy ratio parameter N put opposite effect. Takhar *et al*. (2000) analyzed the combined heat and mass transfer along a vertical moving cylinder with a free stream and deduced that the Prandtl number affects the surface heat transfer while Schmidt number affects the mass transfer. Further, Ganesan and Loganathan (2001, 2002) studied different problems of natural convective flow past the moving vertical cylinder. Abdallah and Zeghmati (2011) presented the analysis of opposing buoyancies on natural convection heat and mass transfer in the boundary layer along a vertical cylinder. They deduced that when Sc < Pr, the concentration layer is much thicker than that of thermal layer and for Pr > Sc the result is exactly opposite.

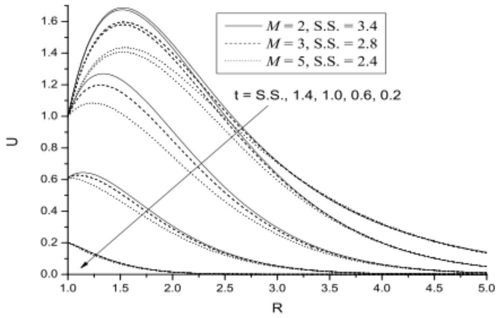


(a) $Gr = 5$, $Gc = 5$, $Sc = 0.6$

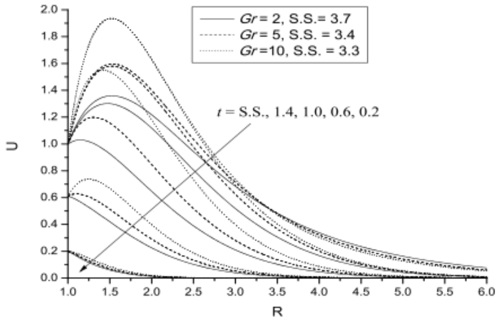


(b) $M = 3$, $Gc = 5$, $Sc = 0.6$

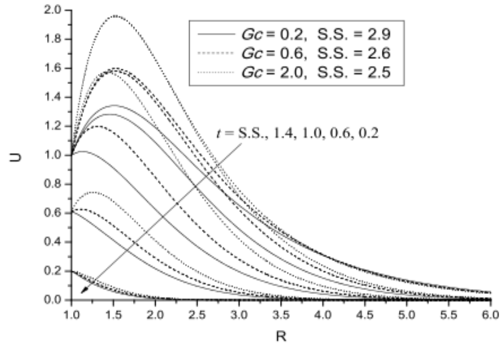


(c) $M = 3$, $Gr = 5$, $Sc = 0.6$

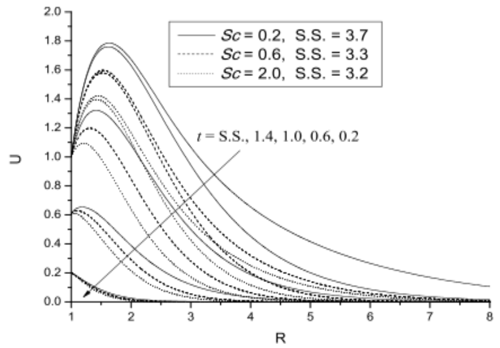


(d) $M = 3$, $Gr = 5$, $Gc = 5$

**Fig. 1. Velocity profiles at a fixed cross-section $X = 0.5$ for different values of $M$, $Gr$, $Gc$ and $Sc$.**

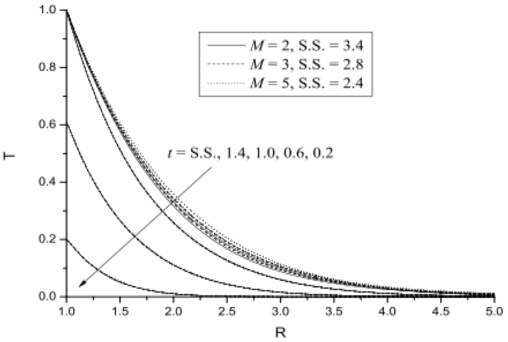


(a) *Gr*= 5, *Gc* = 5, *Sc* = 0.6

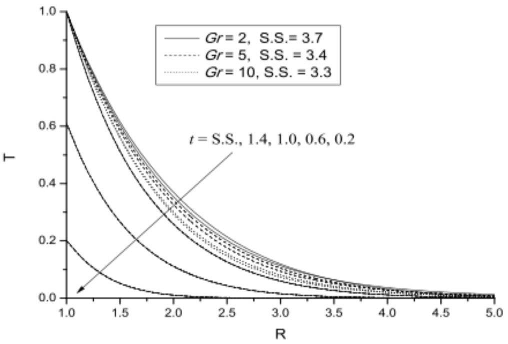


(b) *M*= 3, *Gc* = 5, *Sc* = 0.6

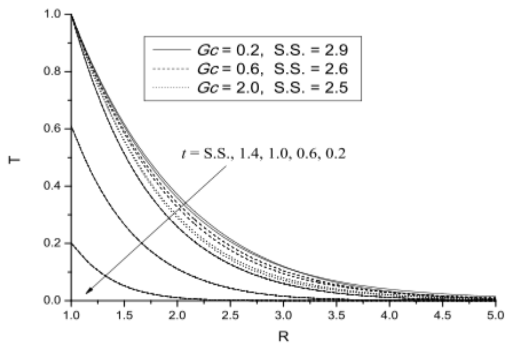


(c) *M*= 3, *Gr* = 5, *Sc* = 0.6

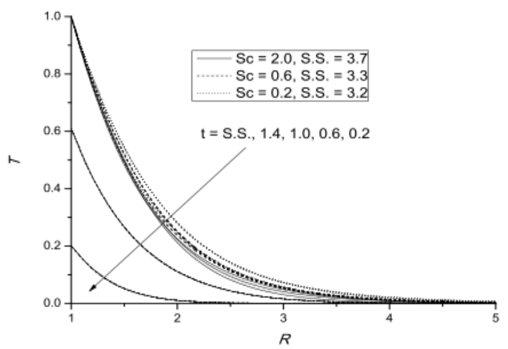


(d) *M*= 3, *Gc* = 5, *Gc* = 5

**Fig. 2. Temperature Profiles at a fixed cross-section *X* = 0.5 for different values of *M, Gr, Gc* and *Sc*.**

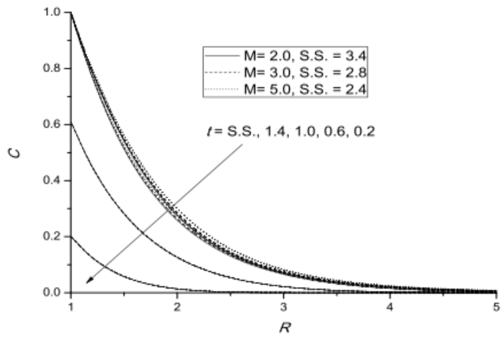


(a) *Gr*= 5, *Gc* = 5, *Sc* = 0.6

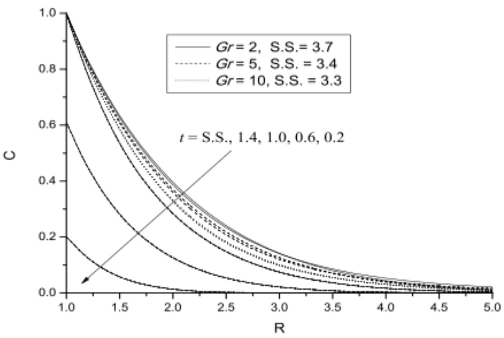


(b) *M*= 3, *Gc* = 5, *Sc* = 0.6

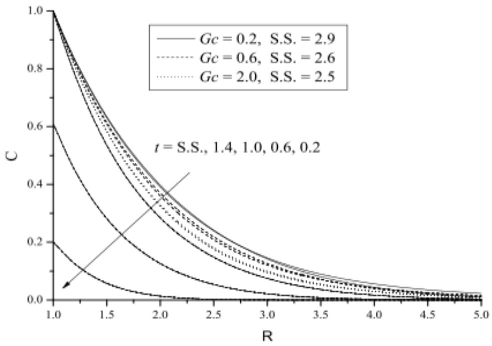


(c) *M*= 3, *Gr* = 5, *Sc* = 0.6

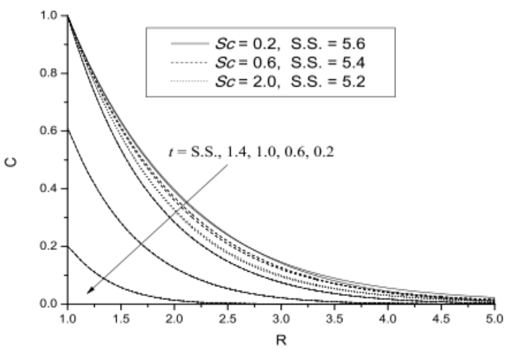


(d) *M*= 3, *Gc* = 5, *Gc* = 5

**Fig. 3. Concentration Profiles at a fixed cross-section X = 0.5 for different values of M, Gr, Gc and Sc.**

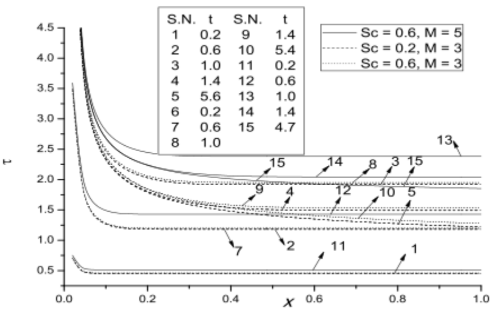


(a) $Gr$=0.4, $Gc$=0.4

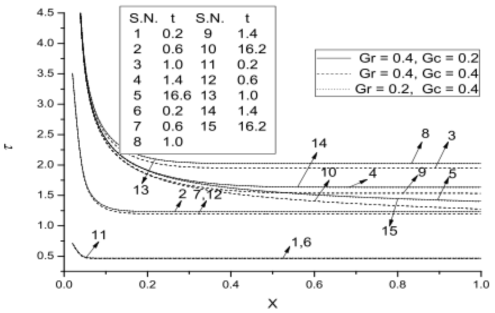


(b) $M$=3, $Sc$=0.6

**Fig. 4. Local Skin-friction Profiles for different values of time parameter.**

The problem of free convection under the influence of a magnetic field has proved to be significant due to its application in geophysics, astrophysics and petroleum industry. In technological processes MHD convection flow problems are important in the field of aeronautics, stellar and planetary magnetosphere, chemical engineering and electronics. Sastry and Bhadram (1987) have analysed the combined free and forced convective flow and heat transfer in vertical annulus by taking into account radial magnetic field. The effect of MHD free convection and mass transfer on the flow past an oscillating infinite coaxial vertical circular cylinder was examined by Raptis and Agarwal (1991). Ganesan and Rani (2000) studied flow behavior on the MHD flow past a vertical cylinder with heat and mass transfer and discussed the unsteady effects of material parameters on the velocity, temperature and concentration. Postelnicu (2004) applied DarcyBoussinesq model to analyze the simultaneous heat and mass transfer by natural convection from a vertical flat plate embedded in electrically conducting fluid saturated porous medium with Soret and Dufour effect and he showed effect of governing parameters on the heat and mass transfer. Reddy and Reddy (2009) investigated the study of radiation and mass transfer effects on unsteady MHD free convection flow of an incompressible viscous fluid past a moving vertical cylinder. They deducted the behavior of the velocity, temperature, concentration, skin-friction, Nusselt number and Sherwood number with variations in the governing thermophysical and hydro-dynamical parameters. Devi and Ganga (2010) discussed the dissipation effects on MHD nonlinear flow and heat transfer past a stretching porous surface under a transverse magnetic field. They concluded that with increase in Eckert number thickness of Thermomagnetic layer increases. Also, Magnetic parameter and suction parameter put retarding effect on the skin friction coefficient at the wall.

The transient free convective MHD flow past an infinite cylinder was studied by Deka and Paul (2013) and they found that the transient velocity increases with Grashof number but decreases with magnetic field parameter. Kumar and Singh (2013) scrutinized the effect of induced magnetic field on natural convection in vertical concentric annuli heated or cooled asymmetrically and gave conclusion that there is rapid decrease in fluid velocity and induced magnetic field with increase in the value of Hartmann number by considering one of the cylinders as conducting compared with the case when both the cylinders are non-conducting. Rani and Reddy (2013) studied the influence of soret and dufour effects on transient double diffusive free convection of couple-stress fluid past a vertical cylinder. They deliberated that increasing values of So or decreasing values of Du increase the average values of skin-friction and heat transfer rate. Reddy (2014) investigated the radiation effects on MHD flow along a vertical cylinder embedded in a porous medium with variable surface temperature and concentration. He deduced that with gain in strength of magnetic field parameter M, the transient velocity decreases while Gr and Gc have opposite effect. Choudhury and Dass (2014) obtained expressions for transient velocity, temperature, species concentration and non-dimensional skin friction at the plate by investigating MHD free convective flow of viscoelastic fluid through porous media in presence of radiation and chemical reaction. Javaherdeh *et al*. (2015) studied the natural convection heat and mass transfer in MHD fluid flow past a moving vertical plate with variable surface temperature and concentration in a porous medium and presented the dimensionless velocity, temperature and concentration profiles as well as gave numerical solution for the local Nusselt number and Sherwood number. His study emphasized on the significance of the relevant parameters. Rajesh *et al*. (2016|) performed the finite difference analysis to study the effect of chemical reaction and temperature oscillation on unsteady MHD free convective flow past a semi-infinite vertical cylinder. They derived graphs for velocity, local as well as average skin-friction, Nusselt number and Sherwood number indicating effects of different physical parameters. Since, free convective flow along vertical cylinder with heat and mass transfer has wide range of applications in the field of geothermal power generation, emergency cooling of a nuclear fuel element by forced circulation in case of power failure, ocean circulations due to heat current and difference in salinity drilling operations etc. In glass and polymer industries, hot filaments, which are considered as a vertical cylinder, are cooled as they pass through the surrounding environment.

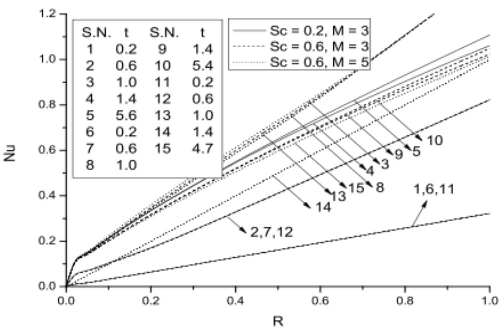


(a) $Gr$=5, $Gc$=5

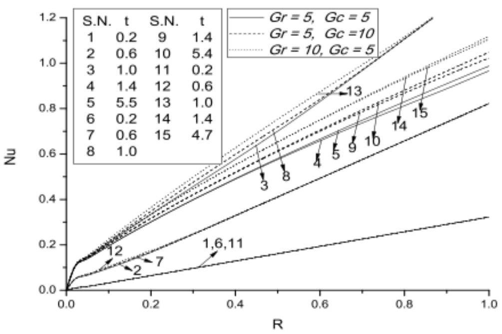


(b) $M$=3, $Sc$=0.6

**Fig. 5. Local Nusselt number Profiles for different values of time parameter.**

In nature, motion starts with constant velocity i.e. $u = 1$, that means when time is increased from zero, the flow gains full velocity which is not possible. Therefore, some researchers start motion by taking $u = t$ which shows that velocity increases with increase in time. But in practical situations, after a long time velocity does not increase with time because it will result in an unstable system. Therefore, we have to deliberate a way in between these two situations which has been invented by taking ramped structures. A significant contribution in the study of ramped velocity was given by Kumar and Singh (2010). The same concept is applied for temperature. When a fluid starts heating, temperature gradually increases but after boiling point temperature becomes constant. This phenomenon is commonly seen in cooling systems like air-conditioner, refrigerators. Kumar and Singh (2011) investigated transient MHD natural convection past a vertical cone having ramped temperature on the curved surface. They presented numerical results for the velocity, temperature, skin-friction and Nusselt number with help of graphs. Recently Das *et al*. (2014) and Seth *et al*. (2016) have done significant studies by considering ramped like temperature profiles. Similar concept is adopted for species concentration.

In present study, we have discussed the analysis of the effect of radial magnetic field on the free convective flow of an electrically conducting and viscous incompressible fluid past a vertical moving cylinder with heat and mass transfer, where the started boundary condition for the temperature, concentration and motion of cylinder are taken as ramped like function. The governing non-linear partial differential equations have been solved numerically by using the implicit finite difference method of Crank-Nicolson type and the results obtained by this study are presented graphically.

## 2. PROBLEM FORMULATION

Consider the transient laminar free convective flow of an electrically conducting and viscous incompressible fluid over a moving vertical cylinder of radius $r_0$ in presence of foreign species. The $x$-axis is taken along the axes of vertical cylinder and $r$-axis is chosen normal to it. A radial magnetic field of the form $B_0 r_0 / r$, which is assumed to be applied transversely to the vertical cylinder and fixed relative to the fluid. The magnetic Reynolds number of the flow is taken to be small enough so that the induced magnetic field can be neglected. Further, the cylinder is assumed to be electrically non-conducting. At the beginning, for $t' \le 0$, the temperature and foreign species concentration at the cylinder are assumed to be $T'_\infty$ and $C'_\infty$ respectively. It is supposed that when time $t' > 0$, the cylinder temperature and species concentration at the cylinder are instantaneously raised or lowered to $T'_\infty + (T'_w - T'_\infty)t'/t_0$ and $C'_\infty + (C'_w - C'_\infty)t'/t_0$ by injection/sublimation respectively and the cylinder is assumed to be moved in the upward direction with velocity $u_0 t'/t_0$ up to time $t' \le t_0$. Further, for $t' \ge t_0$, these are maintained at constant temperature, species concentration and the velocity of the cylinder. For small concentration level, the Soret-Dufour effects can be neglected in the energy equation. Under these assumptions, the physical variables are functions of ($x,r,t'$) only. Then under usual Boussinesq approximation, the governing equations are derived as follows:

$$\frac{\partial (ru)}{\partial x} + \frac{\partial (rv)}{\partial r} = 0, \tag{1}$$

$$\begin{aligned}\frac{\partial u}{\partial t'} + u\frac{\partial u}{\partial x} + v\frac{\partial u}{\partial x} &= g\beta_T (T' - T'_\infty) \\ &+ g\beta_C (C' - C'_\infty) + \frac{\nu}{r}\frac{\partial}{\partial r}\left(r\frac{\partial u}{\partial r}\right) - \frac{\sigma B_0^2 r_0^2 u}{r^2}\end{aligned} \tag{2}$$

$$\frac{\partial T'}{\partial t'} + u\frac{\partial T'}{\partial x} + v\frac{\partial T'}{\partial r} = \frac{\alpha}{r}\frac{\partial}{\partial r}\left(r\frac{\partial T'}{\partial r}\right) \tag{3}$$

$$\frac{\partial C'}{\partial t'} + u\frac{\partial C'}{\partial x} + v\frac{\partial C'}{\partial r} = \frac{D}{r}\frac{\partial}{\partial r}\left(r\frac{\partial C'}{\partial r}\right) \tag{4}$$

The initial and boundary conditions for the considered problem are as follows:

$t' \le 0: u = 0,\ v = 0,\ T' = T'_\infty,\ C' = C'_\infty$ for all $x$ and $r$

$$\begin{cases} u = 0,\ v = 0, \\ T' = T'_\infty,\ C' = C'_\infty, \end{cases} \quad \text{at } x = 0$$

$$t' > 0: \begin{cases} u = u_0 f(t'), \\ T' = T'_\infty + (T'_w - T'_\infty) f(t'), \\ C' = C'_\infty + (C'_w - C'_\infty) f(t'), \end{cases} \quad \text{at } r = r_0$$

$$\begin{cases} u \to 0, T' \to T'_\infty, \\ C' \to C'_\infty \end{cases} \quad \text{as } r \to \infty \tag{5}$$

where

$$f(t') = \begin{cases} t'/t_0 & t' < t_0 \\ 1 & t' \geq t_0 \end{cases}$$

The non-dimensional variables used are as follows:

$$R = \frac{r}{r_0},\ t = \frac{t'}{t_0},\ T = \frac{T' - T'_\infty}{T'_w - T'_\infty},\ \mathrm{C} = \frac{C' - C'_\infty}{C'_w - C'_\infty}$$
$$U = \frac{u}{u_0},\ V = \frac{vt_0}{r_0}\ X = \frac{x}{u_0 t_0},\ t_0 = \frac{r_0^2}{v} \tag{6}$$

By using non-dimensional quantities the governing equations are reduced to following form:

$$\frac{\partial(RU)}{\partial X} + \frac{\partial(RV)}{\partial R} = 0, \tag{7}$$

$$\frac{\partial U}{\partial t} + U\frac{\partial U}{\partial X} + V\frac{\partial U}{\partial R} = \frac{1}{R}\frac{\partial}{\partial R}\left(R\frac{\partial U}{\partial R}\right) + GrT + GcC - \frac{M}{R^2}u \tag{8}$$

$$\frac{\partial T}{\partial t} + U\frac{\partial T}{\partial X} + V\frac{\partial T}{\partial R} = \frac{1}{pr}\frac{1}{R}\frac{\partial}{\partial R}\left(R\frac{\partial T}{\partial R}\right) \tag{9}$$

$$\frac{\partial C}{\partial t} + U\frac{\partial C}{\partial X} + V\frac{\partial C}{\partial R} = \frac{1}{Sc}\frac{1}{R}\frac{\partial}{\partial R}\left(R\frac{\partial C}{\partial R}\right) \tag{10}$$

The initial and boundary conditions in non-dimensional form are obtained as follows:

$t \leq 0: U = 0,\ \mathrm{V} = 0,\ T = 0,\ C = 0$ for all X and R

$$\begin{cases} U = 0,\ V = 0, \\ T = 0,\ C = 0, \end{cases} \quad \text{at } x = 0$$

$$t > 0: \begin{cases} U = f(t),\ T = f(t), \\ C = f(t), \end{cases} \quad \text{at } R = 1$$

$$\begin{cases} U \to 0,\ T \to 0, \\ C \to 0 \end{cases} \quad \text{as } R \to \infty \tag{11}$$

where

$$f(t) = \begin{cases} t & t < 1 \\ 1 & t \geq 1 \end{cases}$$

In the non-dimensional process, we have obtained the following non-dimensional parameters

$$Gr = \frac{g\beta_T r_0^2 (T'_w - T'_\infty)}{vu_0},\ Gc = \frac{g\beta_C r_0^2 (C'_w - C'_\infty)}{vu_0},\ Sc = \frac{v}{D},$$
$$Pr = \frac{v}{\alpha},\ M = \frac{\sigma B_0^2 r_0^2}{\rho v}.$$

## 3. NUMERICAL SOLUTION PROCEDURE

The transport Eqs. (7)-(10) are highly non-linear in nature and their solutions subject to the boundary condition (11) have been obtained numerically. The solutions of the transformed equations have been solved by implicit finite difference method of Crank-Nicolson type. The finite difference equations corresponding to Eqs. (7)-(10) are as follows:

$$\frac{U_{i,j}^{n+1} - U_{i-1,j}^{n+1} + U_{i,j}^{n} - U_{i-1,j}^{n}}{2\Delta X} + \frac{V_{i,j}^{n+1} - V_{i-1,j}^{n+1} + V_{i,j}^{n} - V_{i-1,j}^{n}}{2\Delta R} + \frac{V_{i,j}^{n+1}}{[1 + (j-1)\Delta R]} = 0 \tag{12}$$

$$\begin{aligned} &\frac{U_{i,j}^{n+1} - U_{i,j}^{n}}{\Delta t} + \frac{U_{i,j}^{n}}{2\Delta X}\left(U_{i,j}^{n+1} - U_{i-1,j}^{n} + U_{i,j}^{n} - U_{i-1,j}^{n}\right) \\ &+ \frac{V_{i,j}^{n}}{4\Delta R}\left(U_{i,j+1}^{n+1} - U_{i,j-1}^{n+1} + U_{i,j+1}^{n} - U_{i,j-1}^{n}\right) \\ &= \left(\frac{U_{i,j-1}^{n+1} - 2U_{i,j}^{n+1} + U_{i.j+1}^{n+1} - U_{i,j-1}^{n} - 2U_{i,j}^{n} + U_{i,j+1}^{n}}{2(\Delta R)^2}\right) \\ &+ \left(\frac{U_{i,j+1}^{n+1} - U_{i,j-1}^{n+1} + U_{i,j+1}^{n} - U_{i,j-1}^{n}}{4[1 + (j-1)\Delta R]\Delta R}\right) \\ &+ Gr\left(\frac{T_{i,j}^{n+1} - T_{i,j}^{n}}{2}\right) + Gc\left(\frac{C_{i,j}^{n+1} - C_{i,j}^{n}}{2}\right) \\ &- M\left(\frac{U_{i,j}^{n+1} + U_{i,j}^{n}}{2[1 + (j-1)\Delta R]^2}\right) \end{aligned} \tag{13}$$

$$\begin{aligned} &\frac{T_{i,j}^{n+1} - T_{i,j}^{n}}{\Delta t} + \frac{U_{i,j}^{n}}{2\Delta X}\left(T_{i,j}^{n+1} - T_{i-1,j}^{n} + T_{i,j}^{n} - T_{i-1,j}^{n}\right) \\ &+ \frac{V_{i,j}^{n}}{4\Delta R}\left(T_{i,j+1}^{n+1} - T_{i,j-1}^{n+1} + T_{i,j+1}^{n} - T_{i,j-1}^{n}\right) \\ &= \left(\frac{T_{i,j-1}^{n+1} - 2T_{i,j}^{n+1} + T_{i,j+1}^{n+1} - T_{i,j-1}^{n} - 2T_{i,j}^{n} + T_{i,j+1}^{n}}{2(\Delta R)^2}\right) \\ &+ \left(\frac{T_{i,j+1}^{n+1} - T_{i,j-1}^{n+1} + T_{i,j+1}^{n} - T_{i,j-1}^{n}}{4[1 + (j-1)\Delta R]\Delta R}\right) \end{aligned} \tag{14}$$

$$\begin{aligned} &\frac{C_{i,j}^{n+1} - C_{i,j}^{n}}{\Delta t} + \frac{U_{i,j}^{n}}{2\Delta X}\left(C_{i,j}^{n+1} - C_{i-1,j}^{n} + C_{i,j}^{n} - C_{i-1,j}^{n}\right) \\ &+ \frac{V_{i,j}^{n}}{4\Delta R}\left(C_{i,j+1}^{n+1} - C_{i,j-1}^{n+1} + C_{i,j+1}^{n} - C_{i,j-1}^{n}\right) \end{aligned}$$

$$=\left(\frac{C_{i,j-1}^{n+1}-2C_{i,j}^{n+1}+C_{i,j+1}^{n+1}-C_{i,j-1}^{n}-2C_{i,j}^{n}+C_{i,j+1}^{n}}{2(\Delta R)^2}\right)$$

$$+\left(\frac{C_{i,j+1}^{n+1}-C_{i,j-1}^{n+1}+C_{i,j+1}^{n}-C_{i,j-1}^{n}}{4[1+(j-1)\Delta R]\Delta R}\right) \tag{15}$$

Finally, the Eqs. (12)-(15) are converted into the linear algebraic system and expressed tridiagonally then solved by Thomas algorithm. In the computational procedure, the physical domain is converted into computational domain as a rectangle frame of lines indicating $X_{min}=0$, $X_{max}=1$, $R_{min}=0$ and $R_{max}=20$ where $R_{max}$ corresponds to $R\rightarrow\infty$ which lies very far from the boundary layers. The mesh sizes in the $X$ and $R$ direction are taken as $\Delta X = 0.025$ and $\Delta R = 0.05$ respectively with time step $\Delta t = 0.01$.

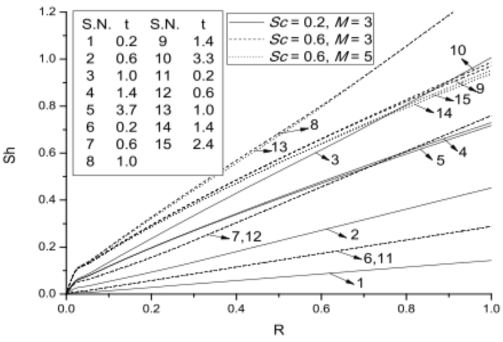


(a) $Gr$=5, $Gc$=5

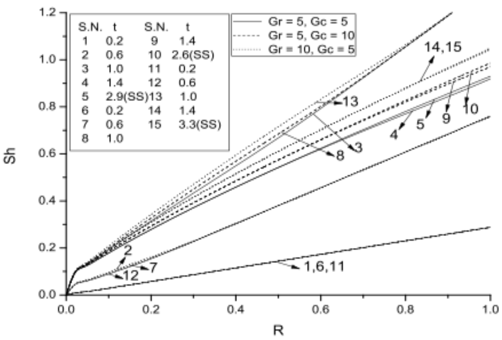


(b) $M$=3, $Sc$=0.6

**Fig. 6. Local Sherwood number Profiles for different values of time parameter.**

During any one time step, the computed values of the previous time step have been used for the coefficients $U$, $T$ and $C$ appearing in Eqs. (12)- (15). At the end of each time step, first we have computed the temperature field and then computed the concentration field and finally the evaluated values are employed to obtain the velocity components in $X$ and $R$ directions respectively .The unsteady values of the components of velocity, temperature field and concentration field for a desired time have been obtained by taking required number of iterations. The steady state numerical solutions have been obtained for the velocity, concentration and temperature fields when the following convergence criterion is satisfied

$$\sum_{i,j}\left|\frac{\Phi_{i,j}^{n+1}-\Phi_{i,j}^{n}}{\Phi_{i,j}^{n+1}}\right|<10^{-5}, \tag{16}$$

where $\Phi_{i,j}^{n}$ stands for either the temperature, velocity or concentration field. The superscripts denote the values of the dependent variables after the nth and ($n$+1)th iterations of time $t$(= $n\Delta t$) respectively, whereas the subscripts $i$ and $j$ indicate grid location in $XR$ plane. Where $X = i\Delta X$ and $R = j\Delta R$ with $\Delta X$, $\Delta R$ and $\Delta t$ the mesh size in $X$, $R$ and $t$ directions respectively for the Eqs. (12)-(16). Other important result of practical importance is the skin-friction, Nusselt number and Sherwood number. By using the computed values of the velocity field, the local skin-friction and the average skin-friction in non-dimensional form are obtained as follows:

$$\tau=-\left.\frac{\partial U}{\partial R}\right|_{R=1}, \tag{17}$$

$$\tau_{av}=-\int_0^1\frac{\partial U}{\partial R}dx. \tag{18}$$

In engineering applications, one of the important characteristic of the flow is the rate of heat and mass transfer over the cone surface. This is estimated by the values of the Nusselt number $Nu$ and Sherwood number $Sh$.

$$Nu=-X\left.\left(\frac{\partial T}{\partial R}\right)\right|_{R=1}, \tag{19}$$

$$Sh=-X\left.\left(\frac{\partial C}{\partial R}\right)\right|_{R=1}, \tag{20}$$

$$Nu_{av}=-\int_0^1\frac{\partial T}{\partial R}dx. \tag{21}$$

$$Sh_{av}=-\int_0^1\frac{\partial C}{\partial R}dx. \tag{22}$$

## 4. RESULT AND DISCUSSION

With a view to see into the physical insight of the problem, numerical computations are carried out for physical parameters involving magnetic parameter $M$, thermal Grashof number $Gr$, mass Grashof number $Gc$, Schmidt number $Sc$ and time parameter $t$ and the numerical solutions are displayed with help of graphs. Fig. 1 represents variation in velocity profiles for different values of the Magnetic Parameter (Fig. 1a), thermal Grashof number Gr (Fig. 1b), mass Grashof number Gc (Fig. 1c) and Schmidt number Sc (Fig. 1d) respectively at a fixed cross-section $X$ =0.5. Fig. 1a depicts that with increase in value of $M$, the velocity profiles decrease. This is due to the fact that when value of $M$ is increased, a resistive type of force is produced known as Lorentz force. This force opposes the motion of the fluid as a consequence velocity decreases. Fig. 1b delineates that with increase in value of *Gr* velocity increases. This happens due to the reason that increasing value of *Gr* will result in increase in Buoyancy force, which accelerates the fluid motion. Therefore, velocity profiles increase. It is observed from Fig. 1c that increase in value of *Gc* will increase the velocity profiles. When the value of *Sc* is increased, velocity profiles get reduced which is shown in Fig. 1d.

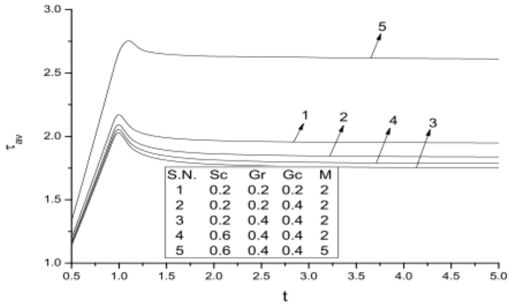


(a) Average Skin-friction

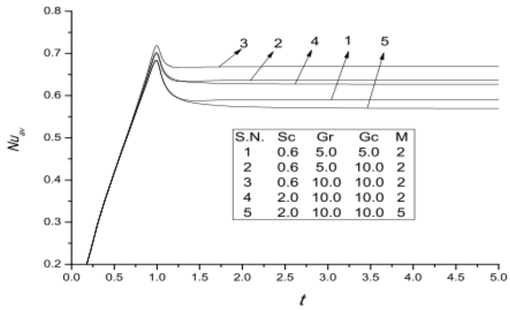


(b) Average Nusselt number

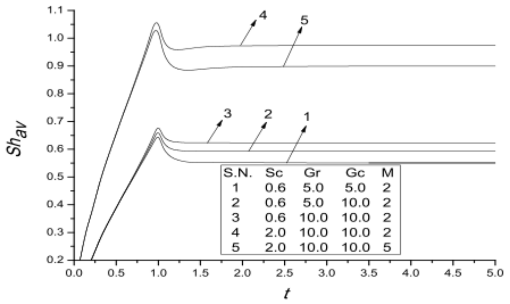


(c) Average Sherwood number

**Fig. 7. Average profiles for different values of *M*, *Gr*, *Gc* and *Sc* w.r.t. time.**

The temperature profiles for different *M*, *Gr*, *Gc* and *Sc* and at a fixed cross-section $X = 0.5$ are plotted in Fig. 2. It is noticed from Fig. 2a that temperature profiles increase with increase in magnetic parameter *M*. Further, time taken to reach the steady-state decrease. There is suppression in temperature profiles with increasing values of *Gr* and *Gc* which is clearly visible in Fig. 2b and 2c. Also, steady-state time decreases with increase in *Gr* and *Gc*. Fig. 2d describes that with increase in value of *Sc*, temperature profiles increase. Fig. 3 illustrates concentration profiles for different values of *M*, *Gr*, *Gc* and *Sc*. Fig. 3a exhibits that with increasing value of M, concentration profiles increases. Further, steady state is achieved earlier with increase in *M*. It is observed from Fig. 3b that concentration profiles get reduced as the value of *Gr* rises up. The species concentration is observed to be high near the surface of the cylinder, decreases continuously with increase in the value of *Gr* and becomes minimum at the end of the boundary layer. From Fig. 3c, we can notice that influence of *Gc* is qualitatively similar to those of *Gr*. As the value of Schimdt number increases, the mass transfer increases and hence the concentration profiles decreases which is shown in Fig. 3d. Also, the steady-state is achieved earlier with increase in all parameters.

In Fig 4 (a)-(b) we have shown the variation in local skin-friction profiles. Fig. 4a reveals that with increase in value of *M* and *Sc*, local skin-friction increases. Fig. 4b shows the influence of *Gr* and *Gc* on local skin-friction profiles. From the Fig. 4b it can be noticed that local skin-friction decreases with increase in *Gr* and *Gc*. Fig 5(a)-(b) presents variation in local Nusselt number. It is observed from the Fig 5a that the local Nusselt number de-creases with an increase in both *M* and *Sc*. From Fig. 5b, we deduce that effect of *Gr* and *Gc* is to enhance the local Nusselt number and hence the heat transfer rate increases. Fig 6a represents the influence of *M* and *Sc* on Sherwood number.

**Table 1 Comparison of average Nusselt Number and average Sherwood Number for ramped case and constant case**

| t | Ramped Case | | Constant Case | |
|---|---|---|---|---|
| | Nu_{av} | Sh_{av} | Nu_{av} | Sh_{av} |
| 0.2 | 0.215087 | 0.197447 | 0.787799 | 0.741577 |
| 0.3 | 0.293729 | 0.271660 | 0.685571 | 0.646670 |
| 0.4 | 0.357678 | 0.332132 | 0.634940 | 0.634940 |
| 0.5 | 0.417269 | 0.388544 | 0.604052 | 0.570208 |
| 0.6 | 0.474086 | 0.442346 | 0.585267 | 0.552171 |
| 0.7 | 0.529288 | 0.494592 | 0.574758 | 0.541715 |
| 0.8 | 0.583875 | 0.546187 | 0.569909 | 0.536444 |
| 0.9 | 0.638818 | 0.598002 | 0.568208 | 0.534090 |
| 1.0 | 0.688952 | 0.651326 | 0.567716 | 0.532920 |
| 1.1 | 0.613412 | 0.578815 | 0.567557 | 0.532154 |
| 1.2 | 0.586882 | 0.553606 | 0.567488 | 0.531563 |
| 1.3 | 0.574237 | 0.541152 | 0.567453 | 0.531087 |
| 1.4 | 0.568779 | 0.535300 | 0.567434 | 0.530695 |
| 1.5 | 0.566919 | 0.532794 | 0.567427 | 0.530370 |
| 2.0 | 0.566983 | 0.530160 | 0.567445 | 0.529360 |
| 2.5 | 0.567256 | 0.529246 | 0.567480 | 0.528871 |
| 3.0 | 0.567387 | 0.528802 | 0.567510 | 0.528602 |
| 3.5 | 0.567460 | 0.528558 | 0.567534 | 0.528440 |
| 4.0 | 0.567503 | 0.528410 | 0.567551 | 0.528334 |
| 4.5 | 0.567532 | 0.528314 | 0.567564 | 0.528263 |
| 5.0 | 0.567551 | 0.528247 | 0.567575 | 0.528211 |
| 5.5 | 0.567566 | 0.528199 | 0.567583 | 0.528172 |
| 6.0 | 0.567577 | 0.528163 | 0.567589 | 0.528143 |
| 6.5 | 0.567585 | 0.528136 | 0.567595 | 0.528121 |
| 7.0 | 0.567592 | 0.528115 | 0.567599 | 0.528103 |

Fig 6a depicts that with increase in value of *Sc* Sherwood number increases while effect of *M* is exactly opposite. It is noticed from Fig 6b that

Sherwood number increases with increase in both *Gr* and *Gc*. Here, the effect is clearly visible for higher values of time. Fig. 7 (a)-(c), depict graphs of average values of skin-friction, Nusselt number and Sherwood number respectively. Fig. 7a reveals that average value of skin-friction increases with increase in *M* and *Sc* but decreases with increase in *Gr* and *Gc*. Fig. 7b delineates that average heat transfer rate get reduced with increase in *Sc* and *M* but enhanced with increase in *Gr* and *Gc*. Fig.7c depicts that average values of Sherwood number decrease with increase in magnetic parameter *M* but all other parameters put adverse effect. One interesting result of our consideration is that all average values of skin-friction, Nusselt number and Sherwood number have increasing trend in time interval (0,1) and thereafter they decreases and finally merge with steady state. The reason behind the increasing trend of these values in interval (0,1) is the ramped nature of boundary conditions.

In order to check the influence of ramped type profiles, we have compared the average values of Nusselt number and Sherwood number corresponding to ramped type boundary conditions for velocity, temperature and concentration with the case of constant boundary condition for velocity, temperature and concentration, which is shown in Table 1. From Table 1, it is clear that in case of ramped type boundary conditions, the values of average Nusselt number and average Sherwood number are low as compared to case of constant boundary conditions. But the steady state values are almost same, achieved at the same time in both the cases. This shows the advantage of taking ramped type boundary conditions, as the heat-transfer rate can be lowered which helps in keeping the system stable. This type of phenomenon can be used in cooling the systems and equipment.

## 5. CONCLUSIONS

The transient free convective flow past a moving vertical cylinder under the influence of radial magnetic field has been studied. The dimensionless governing equations have been solved by using an implicit finite-difference method of Crank-Nicolson type and the results have been presented with help of graphs. By our study, we concluded the following results:

(i) The effect of *M* and *Sc* on velocity profiles is to reduce it as a consequence momentum boundary layer thickness decreases while effect of *Gr* and *Gc* is to enhance it accordingly momentum boundary layer thickness increases.

(ii) The thermal boundary layer expanded with increase in *M* and *Sc* while shrink with increase in *Gr* and *Gc.*

(iii) Concentration profiles rise up with rise in *M* while fall down with increase in all other parameters.

(iv) Local skin-friction increase with increase in *M* and Sc while decrease with increase in *Gr* and *Gc*.

(v) The effect of *M* and *Sc* is to reduce the heat transfer rate while effect of *Gr* and *Gc* is to enhance it.

(vi) With increase in value of *M* Sherwood number decreases while all other parameters have opposite effect.

(vii) Average value of skin-friction decline with increase in magnetic parameter and Schimdt number but thermal Grashof number and mass Grashof have opposite effect.

(viii) Average value of Nusselt number reduces with increase in *M* and *Sc* and while enhances with increase in *Gr* and *Gc*.

(ix) Average value of Sherwood number decreases with increase in magnetic parameter *M* but have exactly opposite behavior with increase in *Gr, Gc* and *Sc*.

(x) With increase in time parameter local and average skin-friction, Nusselt number and Sherwood number increase in time interval (0,1).

## REFERENCES

Abdallah, M. S. and B. Zeghmati (2011). Natural convection heat and mass transfer in the boundary layer along a vertical cylinder with opposing buoyancies. *J. Appl. Fluid Mech.* 4(4), 15-21.

Chen, T. S. and C. F. Yuh (1980). Combined heat and mass transfer in natural convection along a vertical cylinder. *Int. J. Heat Mass Transf.* 23, 451-461.

Choudhury, R. and S. K. Das (2014). Viscoelastic MHD free convective flow through porous media in presence of radiation and chemical reaction with heat and mass transfer. *J. Appl. Fluid Mech.* 7(4), 603-609.

Das, M., B. K. Mahatha, R. Nandkeolyar, B. K. Mandal and K. Saurabh (2014). Unsteady hydromagnetic flow of a heat absorbing dusty fluid past a permeable vertical plate with ramped temperature. *J. Appl. Fluid Mech.* 7(3), 485-492.

Deka, R. and A. Paul (2013). Transient free convective MHD flow past an infinite vertical cylinder. *Theo. Appl. Mech.* 40, 385-402.

Devi, S. A. and B. Ganga (2010). Dissipation effects on MHD nonlinear flow and heat transfer past a porous surface with prescribed heat flux. *J. Appl. Fluid Mech.* 3(1), 1-6.

Ganesan, P. and H. P. Rani (1998). Transient natural convection along vertical cylinder with Heat and Mass transfer. *Heat Mass Transf.* 33, 449-456.

Ganesan, P. and P. Loganathan (2001). Effects of mass transfer and flow past a moving vertical cylinder with constant heat flux. *Acta Mach.*

150, 179-190.

Ganesan, P. and P. Loganathan (2002). Heat and mass flux effects on a moving vertical cylinder with chemically reactive species diffusion. *J. Eng. Phy. Thermophy*. 75, 899-909.

Ganesan, P. G. and H. P. Rani (2000). Unsteady free convection MHD flow past a vertical cylinder with heat and mass transfer. *Int. J. Therm. Sci.* 39, 265-272.

Gorla, R. S. R. (1989). Combined forced and free convection in the boundary layer flow of a micropolar fluid on a continuous moving vertical cylinder. *Int. J. Eng. Sci*. 27, 77-86.

Javaherdeh, K., M. Mirzaei Nejad and M. Moslemi (2015). Natural convection heat and mass transfer in MHD fluid flow past a moving vertical plate with variable surface temperature and concentration in a porous medium. *Eng. Sci. Tech. An Int. J*. 18, 423-431.

Kumar, A. and A. K. Singh (2010). Transient magnetohydrodynamic couette flow with ramped velocity. *Int. J. Fluid Mech. Res.* 37, 435-446.

Kumar, A. and A. K. Singh (2011). Transient MHD natural convection past a vertical cone having ramped temperature on the curved surface. *Int. J. Energy Tech.* 3, 1-6.

Kumar, A. and A. K. Singh (2013). Effect of induced magnetic field on natural convection in vertical concentric annuli heated/cooled asymmetrically. *J. Appl. Fluid Mech.* 6, 15-26.

Lien, F. S., Ch. Chen and Y. M. Chang (1985). Effect of free convection and mass transfer on the flow past an impulsively moving infinite vertical circular cylinder. *Int. Comm. Heat Mass Transf.* 12, 127–137.

Postelnicu, A. (2004). Influence of a magnetic field on heat and mass transfer by natural convection from vertical surfaces in porous media considering Soret and Dufour effect. *Int. J. Heat Mass Transf.* 47, 1467–1472.

Rajesh, V., O. A. Bég and C. Sridevi (2016) Finite difference analysis of un-steady MHD free convective flow over moving semi-infinite vertical cylinder with chemical reaction and temperature oscillation effects. *J. Appl. Fluid Mech.* 9(1), 157-167.

Rani, H. P. and G. J. Reddy (2013) Soret and dufour effects on transient double diffusive free convection of couple-stress fluid past a vertical cylinder. J. Appl. Fluid Mech. 6(4), 545-554.

Raptis, A. and A. K. Agarwal (1991). Effect of MHD free convection and mass transfer on the flow past an oscillating infinite coaxial vertical circular cylinder. *Warmeund Stoffubetragung* 26, 253-256.

Reddy, M. G. (2014). Radiation effects on MHD flow along a vertical cylinder embedded in a porous medium with variable surface temperature and concentration. *Frontiers Heat Mass Transf.* 5(4), 1-9.

Reddy, M. G. and N. B. Reddy (2009). Radiation and mass transfer effects on unsteady MHD free convection flow of an incompressible viscous fluid past a moving vertical cylinder. *Theo. Appl. Mech.* 36, 239–260.

Sastry, V. U. K. and C. V. V. Bhadram (1987). Hydromagnetic convective heat transfer in vertical pipes. *Appl. Sci. Res*. 34, 117-125.

Seth, G. S., R. Sharma and B. Kumbhakar (2016). Effects on unsteady MHD natural convection flow of a chemically reactive and radiating fluid through a porous medium past a moving vertical plate with arbitrary ramped temperature. *J. Appl. Fluid Mech.* 9(1), 103-117.

Sparrow, E. M. and J. L. Gregg (1956). Laminar free convection heat transfer from the outer surface of a vertical circular cylinder. *Trans. ASME* 78, 1823-1829.

Takhar, H. S., A. J. Chamkha and G. Nath (2000). Combined heat and mass transfer along a vertical moving cylinder with a free stream. *Heat and Mass Transf*. 36, 237-246.

Velusamy, K. and V. K. Garg (1992). Transient natural convection over a heat generating vertical cylinder. *Int. J. Heat Mass Transf.* 35, 1293-1306.

Yang, K. T. (1960). Possible similarity solutions for laminar free convection on vertical plates and cylinders. *J. Appl. Mech.* 27, 230-236.